COMPARISON OF $POCL_3$ & BBR_3 FURNACE DIFFUSSION DOPANT SOURCES TO PHOSPHORUS & BORON IMPLANT AND PLASMA DOPANT SOURCES FOR SELECTIVE EMITTER FORMATION USING LOCALIZED LASER MELT (LLM) ANNEALING EITHER BEFORE OR AFTER SIN/ARC

John Borland[1], John Chen[2], Peter Oesterlin[3], Peter Venema[4], Henri Geerman[4], Yao-Jen Lee[5], Peter Zhao[6], Larry Wang[6], Baomin Xu[7] and Shu Qin[8]
[1]JOB Technologies, Aiea, Hawaii, USA
[2]Kingstone, Shanghai, China
[3]Innovavent GmbH, Gottingen, Germany
[4]Tempress Systems B.V., Vaassen, the Netherlands
[5]National Nano Device Labs, Hsinchu, Taiwan
[6]Eavans Analytical Group, Sunnyvale, California, USA
[7]PARC, Palo Alto, California, USA
[8]Micron Technology, Boise, Idaho, USA

ABSTRACT: We compared $POCl_3$ and BBr_3 furnace diffused dopant source to phosphorus and boron implanted dopant as well as BF_3 and arsenic plasma implant dopant sources for selective emitter junction formation with laser annealing and emitter field junction formation with RTA, furnace and microwave annealing all either before or after SiN/ARC. Localized laser melt (LLM) annealing for liquid phase selective emitter dopant diffusion at 3, 5 and 6.5 J/cm^2 resulted in textured wafer junction depths of 1.8um, 2.6um and 3.5um respectively and Rs as low as 7.0Ω/□. LLM after SiN/ARC resulted in a 2x degradation in Rs dopant activation. Nitrogen SIMS depth profile showed high levels of N in the E19 to E20/cm^3 incorporated in the melt region while oxygen incorporation in the melt region was much lower at <5E18/cm^3. Also, furnace 1st then LLM annealing sequence results in 30-44% lower dopant activation compared to LLM 1st then furnace annealing sequence.
Keywords: Doping, Implantation, Laser Processing, Selective Emitter

1 INTRODUCTION

The PV industry is focused on developing higher efficiency solar cells with tighter distribution which will lead to higher binning yields (less rejects) and higher power solar panel modules. There are a number of key process technologies to achieve higher efficiency cells and tighter binning such as advanced metallization, selective emitter, dielectric passivation, back contact etc. In this paper we will focus on the selective emitter approach.

The basic concept for selective emitter (SE) as shown in Fig.1 from simulations reported by Borland et al. is to have a very high lifetime n/p junction surface region to reduce recombination where the light is absorbed forming electron hole pairs [1]. This is the emitter field (EF) region located between the front surface metal lines (emitter finger). The doping level in this region needs to be low at <2E19/cm^3 for Rs >120Ω/□. However, in the SE metal contact region where the light is shadowed by the metal finger lines so lifetime is not an issue you want low contact resistance and high dopant level >2E20/cm^3 for low Rs <30Ω/□.

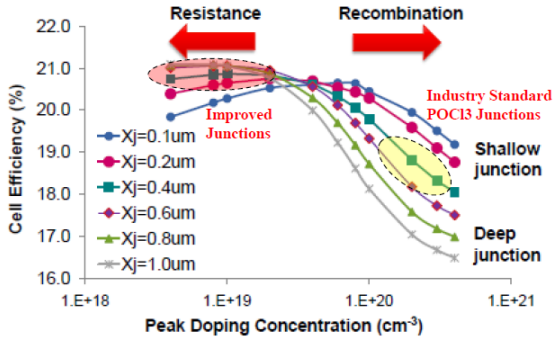

Fig.1: Simulation results for cell efficiency based on surface doping concentration [1].

A simple implementation of selective emitter is to use standard $POCl_3$ diffusion furnace doping followed by screen printing a wax over the emitter finger region and etch back the silicon surface to reduce the phosphorus surface level to <2E19/cm^3. Nejatiet et al. reported on a new method using a screen printed paste that etches PSG at room temperature so they could realize a 100Ω/□ emitter field region with a 50Ω/□ selective emitter region for metal contact at PVSC-2012 [2]. This improved both cell efficiency and distribution (binning) from 18.3% +/- 0.4% to 18.8% +/-0.2%.

Another method to form selective emitter is to use silicon-ink doped with phosphorus called Cougar as first reported by Burrows et al. [3] and Liu et al. [4]. The phosphorus doped Si-ink gives a surface doping level of 2-5E20/cm^3 (10-50Ω/□) for the selective emitter contact region while $POCl_3$ is used to achieve a 2-9E19/cm^3 emitter field dopant level (90-120Ω/□). The efficiency improved from 17.9% to 18.9% as reported by Innovalight at PVSC-2010 [5 & 6].

The localized laser melt (LLM) method for selective emitter formation also called laser doped selective emitter (LDSE) does not need screen-printing so is mask free forming the selective emitter doped finger line structures as reported by Jaeger et al. [7]. Using $POCl_3$ diffusion to achieved a 120Ω/□ (5E14/cm^2 phosphorus dopant concentration emitter field region) the LLM process improves Rs to <23Ω/□ (4E15/cm^2 activated phosphorus dopant concentration SE region).

2 EXPERIMENTATION

In this study we compared n-type phosphorus doping by $POCl_3$ diffusion furnace to phosphorus beam-line implantation and arsenic plasma implantation for n-type junctions while for p-type junctions we compared BBr_3 diffusion furnace to B beam-line implantation and BF_3

plasma implantation for boron doping. Dopant annealing and diffusion was achieved by; 1) 515nm green laser annealing with 300ns pulse duration at Innovavent in Germany, 2) 500°C microwave annealing at Nano Device Lab in Taiwan, 3) 750°C-1050°C horizontal tube furnace annealing at Tempress in the Netherlands and 4) 650°C-1050°C rapid thermal annealing at Nano Device Lab in Taiwan.

2.1 Part 1 selective emitter formation before SiN/ARC

Part 1 involved looking at selective emitter implant doping before SiN/ARC over the phosphorus and boron dose range of 3E14/cm^2 to 1.0E16/cm^2 at either 15keV or 30keV implant energies as shown in Fig.2. These wafers were implanted by Kingstone in Shanghai, China. Tempress in the Netherlands provided the standard $POCl_3$ and BBr_3 diffusion furnace doped wafers for comparison. Microwave annealing at about 500°C was performed by National Nano Device Labs in Taiwan, furnace annealing at 750°C, 850°C and 1050°C by Tempress and LLM annealing at >1407°C by Innovavent in Germany.

Species	Dose	Energy	Microwave	750C	850C	1050C	Laser=1J	3J	5J	6.7J
B	3E14	15keV	X	X	X	X	X	X	X	X
B	3E14	30keV	X	X	X	X	X	X	X	X
B	1E15	15keV	X	X	X	X	X	X	X	X
B	1E15	30keV	X	X	X	X	X	X	X	X
B	3E15	15keV	X	X	X	X	X	X	X	X
B	3E15	30keV	X	X	X	X	X	X	X	X
B	1E16	15keV	X	X	X	X	X	X	X	X
B	1E16	30keV	X	X	X	X	X	X	X	X
P	3E14	15keV	X	X	X	X	X	X	X	X
P	3E14	30keV	X	X	X	X	X	X	X	X
P	1E15	15keV	X	X	X	X	X	X	X	X
P	1E15	30keV	X	X	X	X	X	X	X	X
P	3E15	15keV	X	X	X	X	X	X	X	X
P	3E15	30keV	X	X	X	X	X	X	X	X
P	1E16	15keV	X	X	X	X	X	X	X	X
P	1E16	30keV	X	X	X	X	X	X	X	X
POCl3	→						X	X	X	X
BBr3	→						X	X	X	X

Fig.2: Part 1 experimental matrix.

2.2 Part 2 higher implant dose selective emitter formation wafers.

From the results in part 1 we could determine that the P dopant source level in standard $POCl_3$ was ~1.1E16/cm^2 and B dopant reported from B-SOD was >1.7E16/cm^2 so we decided to look at implant doses > 3.0E16/cm^2. This required plasma implantation because beam-line implantation times would be too long. Micron provided BF_3 and AsH_3 plasma doped wafers at 10kV and 4E16/cm^2 dose. These wafers were LLM by Innovavent at 1.0, 3.0, 5.0 and 6.5 J/cm^2 on the top half of the wafers as shown in Fig.3 while NDL did both microwave annealing and RTA annealing at 1000°C for 10sec and 60sec and 1050°C for 60sec on the bottom half of the wafers. The experimental matrix is shown in Fig.4.

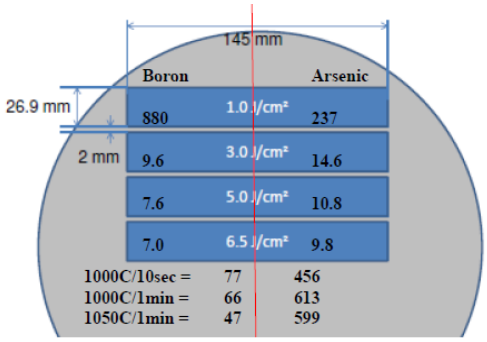

Fig.3: Plasma implant wafer laser annealing pattern.

Species	Dose	Energy	Laser= 1J	3J	5J	6.5J	RTA/60 sec
B-PLAD	4E16	10kV	X	X	X	X	X
As-PLAD	4E16	10kV	X	X	X	X	X
SiN/B	3E15	15keV	X	X	X	X	X
SiN/P	3E15	15keV	X	X	X	X	X

Fig.4: Part 2 & 3 experimental matrix.

2.3 Part 3 implanted selective emitter formation after SiN/ARC wafers

Part 3 involved getting implanted SiN/ARC textured 156mm solar wafers. This is our alternative to the P-dopant source on top of the SiN/ARC reported by Suntech-power Pluto cell [8] and the in-situ doped SiN/ARC reported by Paviet-Salomon et al. [9]. Solar textured wafers that had P & B implants at 15keV and 3E15/cm^2 dose with a 78nm SiN/ARC coating were processed as shown in Fig.5. Innovavent performed the selective emitter SiN ablation and liquid phase melt dopant diffusion of the SiN wafers by LLM with power densities from 2.75J/cm^2 to 6.5J/cm^2 at 0.25J/cm^2 increasing laser power levels as shown in Fig.5. NDL performed RTA and microwave annealing on the non-LLM regions to simulate dopant diffusion in the emitter field region.

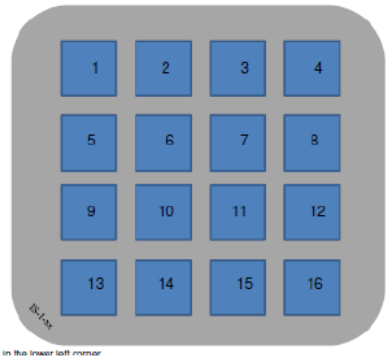

area	energy density (J/cm²)	area	energy density (J/cm²)
1	2.75	9	4.75
2	3.0	10	5.0
3	3.25	11	5.25
4	3.5	12	5.5
5	3.75	13	5.75
6	4.0	14	6.0
7	4.25	15	6.25
8	4.5	16	6.5

Fig.5: SiN/implant wafer laser annealing pattern for SiN ablation and localized laser melt annealing.

3 RESULTS

3.1 Part 1 and 2 results for selective emitter and emitter field P-implant junction formation before SiN/ARC.

Fig.6 shows the Rs versus laser power levels for $POCl_3$ diffusion, P-implant and As-plasma implant conditions. The 1J/cm^2 laser power level only activated about 3% of the high dose As-plasma implant wafer (Rs=237Ω/□ activated dose =2.5E14/cm^2) shown in Fig.7. All of the other P-implant dose Rs values were too high to measure and the $POCl_3$ Rs value was the same as the non-laser anneal sample of 68Ω/□. At 3J/cm^2 and higher laser power levels we achieve 100% dopant activation as shown in Figs.6 & 7. Fig.7 also shows the Rs results for the other annealing methods including 500°C microwave annealing, 1000°C RTA annealing and furnace annealing at 750°C, 850°C and 1050°C. Note that for the low temperature microwave and 750°C

furnace anneal conditions Rs saturates at about 100Ω/□ for the 15keV P-implant and at 30keV Rs saturates at 50Ω/□ for doses >2E15/cm^2. Kennel reported that P dopant activation is limited by solid solubility and at 750°C that is ~2.0E20/cm^3 [10].

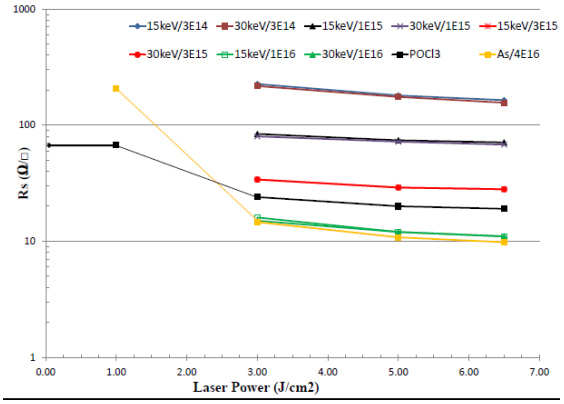

Fig.6: $POCl_3$, phosphorus and arsenic implant Rs results at various laser power conditions.

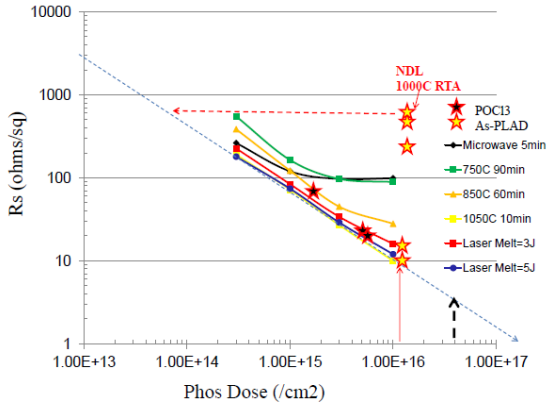

Fig.7: Rs versus 15keV P-implant dose for various annealing methods.

SIMS analysis by EAG for the $POCl_3$ samples are shown in Fig.8. The green P and O SIMS profiles are for standard $POCL_3$ diffusion. The red profiles are for the 3J/cm^2 laser anneal and the purple profiles are for the 5J/cm^2 laser anneal. The 68Ω/□ Rs value corresponds to a P activated level of 2.0E15/cm^2 from Fig.7 but the SIMS total P areal density (P-AD) is 1.08E16/cm^2 and P-AD in silicon is 4.4E15/cm^2 therefore only ~20% of the total P dopant is electrically active. After the laser anneal at 3J/cm^2 or greater Rs decreases to 20-23Ω/□ corresponding to 100% P dopant activation at a P concentration level of 5.5E15/cm^2 from SIMS P-AD and Fig.7 Rs versus P implant dose. Note the O-SIMS profile shows oxygen liquid phase diffusion to the melt depth and level of <5E18/cm^3 with O areal density of 0.8-1.8E17/cm^2.

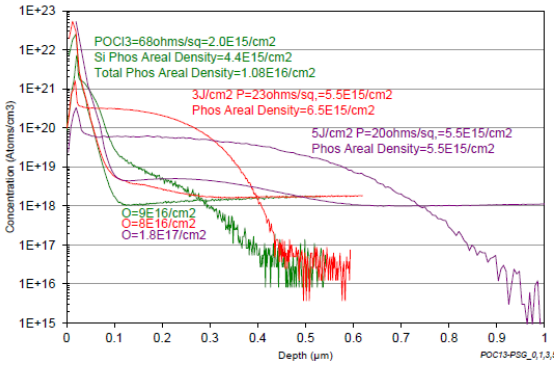

Fig.8: $POCl_3$ P and O SIMS areal density results.

The 15keV P-implant at 3E14/cm^2 and 1E16/cm^2 doses P-SIMS results are shown in Fig.9 for as implanted no anneal, 3J/cm^2 and 5J/cm^2 laser anneals. 100% P dopant activation is realized for these laser anneals and the SIMS P-AD are in good agreement to the target doses. As shown earlier in Fig.6 no P dopant activation was seen for the 1J/cm^2 laser anneal condition.

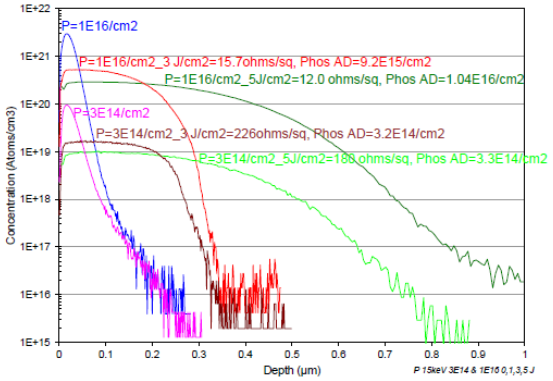

Fig.9: P-implant at 15keV 3E14/cm^2 and 1E16/cm^2 dose P-SIMS areal density analysis.

The 10kV As-plasma implant at 4E16/cm^2 dose SIMS results are shown in Fig.10. Note that the actual SIMS As-dopant areal density is ~1.2E16/cm^2 instead of the targeted 4E16/cm^2. At 1J/cm^2 Rs was 237Ω/□ which corresponds to an activated dose of only 2.5E14/cm^2 or 2% activation as shown in Fig.7. For the 3J/cm^2 or higher laser power 100% As dopant activation is realized. NDL did 1000°C RTA anneal resulting in very high Rs values of >450Ω/□ as shown in Fig.7 corresponding to <0.5% activated dose of ~7E13/cm^2.

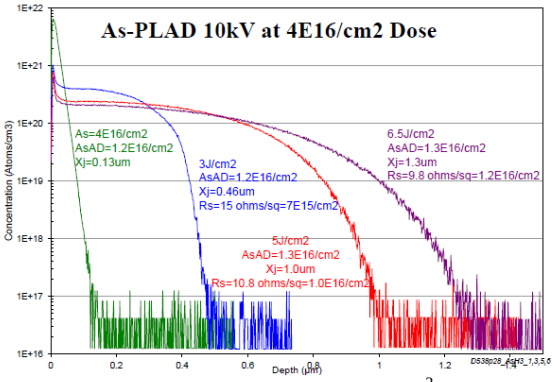

Fig.10: 10kV As-plasma implant at 4E16/cm^2 dose SIMS areal density analysis.

For the EF junction target of >100Ω/□, a 500°C microwave or <750°C furnace anneal for the 15keV P-implant at any dose between 3E14/cm^2 to 1E16/cm^2. For SE junction target of <20Ω/□ P-implant of >1E16/cm^2 dose with 3J/cm^2 or higher laser power condition is required.

3.2 Part 1 & 2 results for SE and EF boron implant junction formation before SiN/ARC.

Similar to Fig.6, Fig.11 shows the Rs versus laser power levels for BBr_3 diffusion, B-implant and BF_3-plasma implant conditions. Again only the plasma implant case shows some dopant activation for the 1J/cm^2 laser anneal. BF_3-plasma Rs=880Ω/□ corresponding to an activated dose of 9E13/cm^2 or ~0.25% as shown in Fig.12.

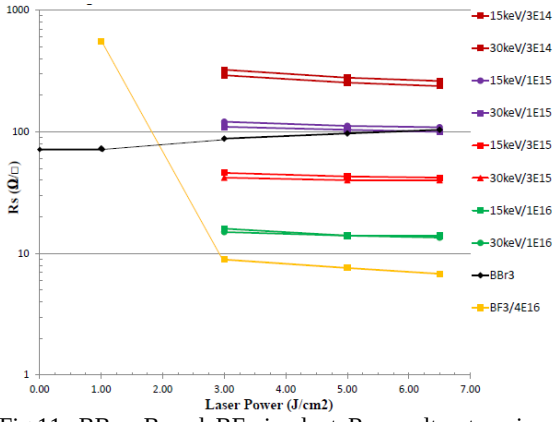

Fig.11: BBr_3, B and BF_3 implant Rs results at various laser power conditions.

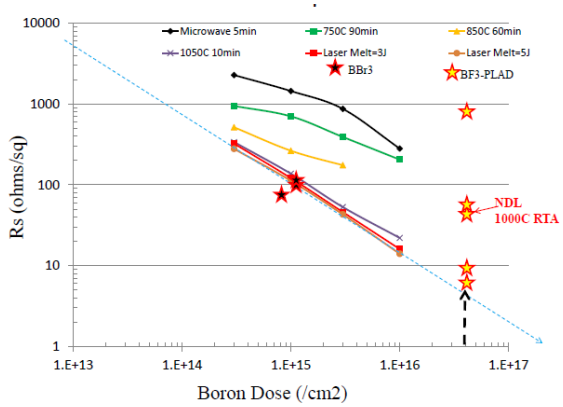

Fig.12: Rs versus 15keV B-implant dose for various annealing methods.

The BBr_3 B-SIMS results are shown in Fig.13, the Rs=77Ω/□ corresponding to a B activated concentration/dose of 1.5E15/cm^2 but the SIMS B areal density (B-AD) was only 8.5E14/cm^2. The SIMS B-AD is based on 11B and there can be other B elemental species such as 10B etc. which can account for the 6.5E14/cm^2 dose difference. This might also explain the surprising result in Fig.11 showing increasing Rs with increasing laser power for the BBr_3 sample case going from 77Ω/□ (B activated dose=1.5E15/cm^2) at 0 and 1J/cm^2 to 88Ω/□ (B activated dose=1.2E15/cm^2) at 3J/cm^2 then 97Ω/□ (B activated dose=1.1E15/cm^2) at 5J/cm^2 and finally to 104Ω/□ (B activated dose=9.5E14/cm^2) at 6.5J/cm^2.

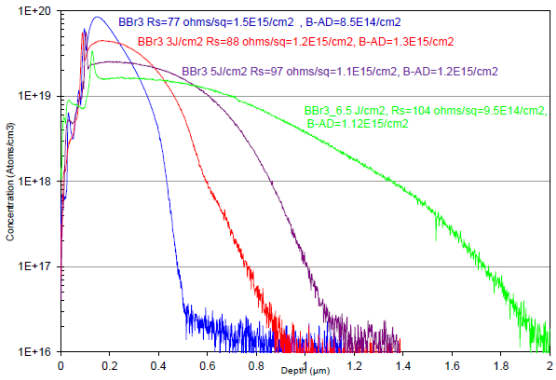

Fig.13: BBr_3 11B-SIMS areal density analysis.

B-implant at 15keV at 3E14/cm^2 and 1E16/cm^2 dose SIMS results are shown in Fig.14. B-AD for the 1E16/cm^2 implant shows that only ~70% of the target B dose was implanted into the silicon for a retained dose of 7E15/cm^2. The B-AD for the 3J/cm^2 case was 7.3E15/cm^2 and Rs=16Ω/□. For B=3E14/cm^2, 3J/cm^2 Rs=324Ω/□ and B-AD=2.7E14/cm^2 while for 5J/cm^2 Rs=279Ω/□ and B-AD=2.9E14/cm^2.

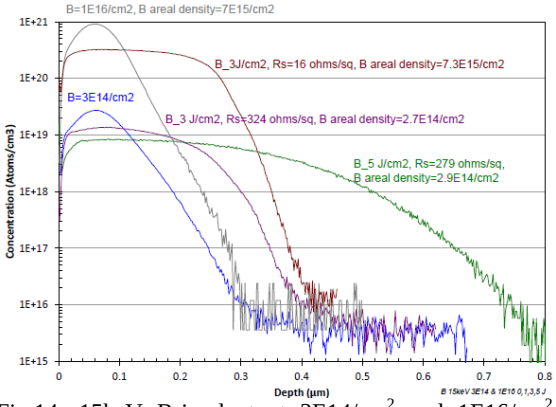

Fig.14: 15keV B-implant at 3E14/cm^2 and 1E16/cm^2 dose B-SIMS areal density analysis.

Fig.15 shows the 11B SIMS results for 10kV BF_3-plasma implant (PLAD) at 4E16/cm^2 dose. Since plasma implant is also not mass analyzed similar to BBr_3 there can be other mixtures of B and not just 11B implanted into the silicon and this could explain why the B activated dose is higher than the 11B areal density. The 3J/cm^2 Rs=9.6Ω/□ for B activated dose of 1.8E16/cm^2 but SIMS B-AD was only 1.3E16/cm^2. At 5J/cm^2, Rs=7.6Ω/□ for activated dose of 2.0E16/cm^2 but B-AD was 1.3E16/cm^2. At 6.5J/cm^2 Rs=7.0Ω/□ for activated dose of 2.5E16/cm^2 but B-AD was 1.0E16/cm^2. These results suggest we should also look into ECV measurements in the future for comparison. The 1000°C RTA anneal results are also shown in Fig.12, Rs results shows ~10% B dopant activation with an activated dose of ~3E15/cm^2.

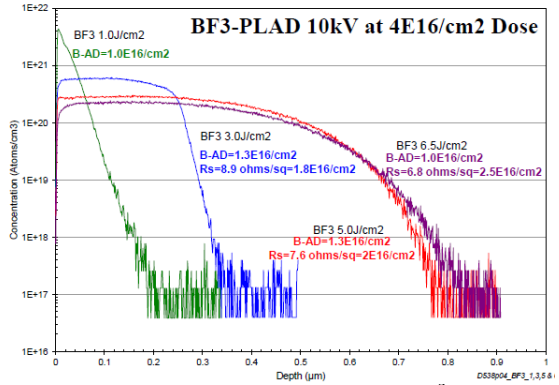

Fig.15: 10kV BF_3-plasma implant at 4E16/cm^2 dose 11B-SIMS areal density analysis.

For the EF junction target of >100Ω/□, any of the low furnace anneals at <1E16/cm^2 B dose can be used. For SE junction target of <20Ω/□ B-implant of >1E16/cm^2 dose with 3J/cm^2 or higher laser power condition is required.

3.3 Part 3 results for SE and EF P & B implant junction formation after SiN/ARC.

As shown earlier in Fig.5 the optical photomicrographs of the SiN textured wafers from region #2 (3J/cm^2), region #10 (5J/cm^2) and region #16 (6.5J/cm^2) are shown in Fig.16. Complete SiN removal was achieved at the low 3J/cm^2 laser power level with some random residual surface texture remaining while at 5J/cm^2 complete surface laser polishing can be seen with no evidence of surface texturing in region #10.

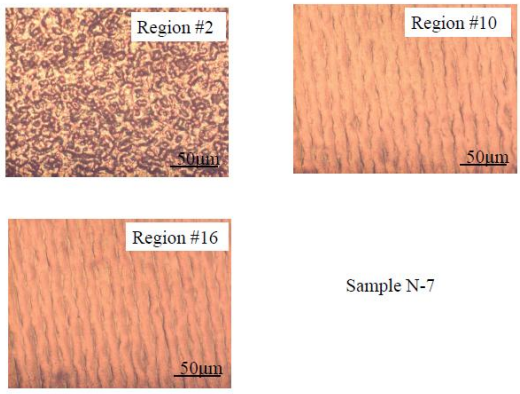

Fig.16: Optical micrographs of 3.0, 5.0 and 6.5 J/cm^2 laser annealed regions showing SiN removal and melted silicon textured surface from Fig.5.

Fig.17 and 18 shows the Rs versus laser power for the 15keV P and B implants at 3E15/cm^2 dose with or without the surface SiN/ARC. For all the laser annealing conditions with a surface SiN/ARC for both P and B implant the Rs values always increased rather than decrease so that at 6.5J/cm^2 P-implant Rs=28Ω/□ and SiN/P-implant Rs=44Ω/□ while B-implant Rs=42Ω/□ and SiN/B-implant Rs=80Ω/□. Even though the SIMS SiN/P-AD is 2.8E15/cm^2 as shown in Fig. 19 the activated P is only 1.9E15/cm^2 for Rs=44Ω/□. The SiN/B-AD is shown in Fig.20 and for 6.5J/cm2 was 2.1E15/cm^2 with an Rs=80Ω/□ for a B activated dose of 1.5E15/cm^2 or 30% drop in activated B & P concentration. To examine this further we decided to also look at both nitrogen (N) and oxygen (O) SIMS analysis. Xu et al. of PARC showed that selective laser drilling to ablate/remove an 80nm SiN/ARC resulted in N diffusion into silicon to a depth of 150nm requiring multiple laser pulses to reduce the N-level [11].

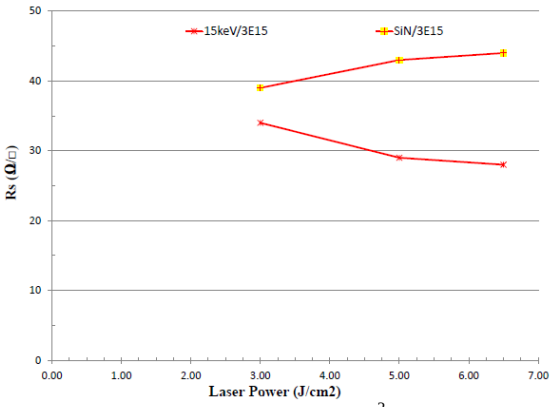

Fig.17: 15keV P-implant at 3E15/cm^2 dose Rs results comparing various laser annealing conditions either before or after SiN/ARC.

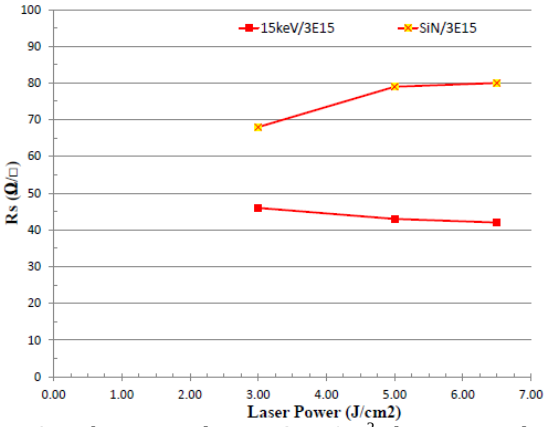

Fig.18: 15keV B-implant at 3E15/cm^2 dose Rs results comparing various laser annealing conditions either before or after SiN/ARC.

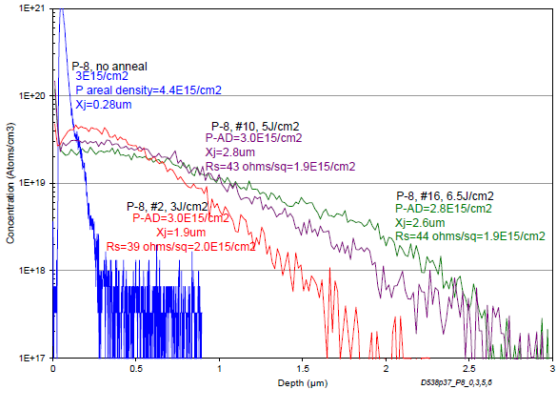

Fig.19: SiN/P-implant P-SIMS areal density analysis.

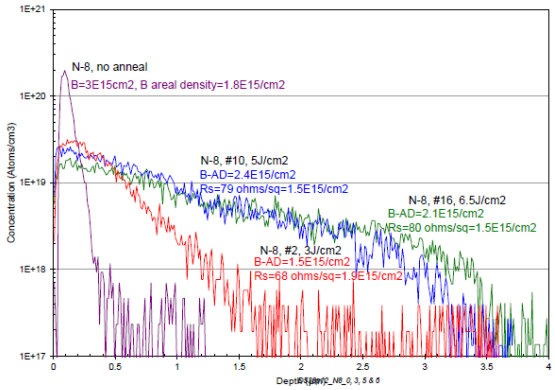

Fig.20: SiN/B-implant B-SIMS areal density analysis.

Fig.21 shows the N-SIMS analysis with the N-AD along with the P-SIMS results for comparison. The N-AD was high at 2.8-4.5E16/cm^2 even after laser ablation or melt removal of the surface SiN layer. Most interesting was the N-SIMS depth profiles which shows N incorporation levels in the silicon melt region in the E19 to E20/cm^3 range which is more than an order of magnitude above the P dopant level at 2-5E19/cm^3. Fig.22 shows the SiN/B N-SIMS results. Again the N level in the melt region is more than an order of magnitude higher than the B level. Therefore in the future we recommend looking at >1E16/cm^2 P and B implant doses so the N level in the melt will have no degradation effect on both P and B dopant activation levels as shown in Fig. 17 and 18. We also observed that at the same laser power level the melt depth for textured surface is 4x deeper than polished silicon surface as shown in Fig.23.

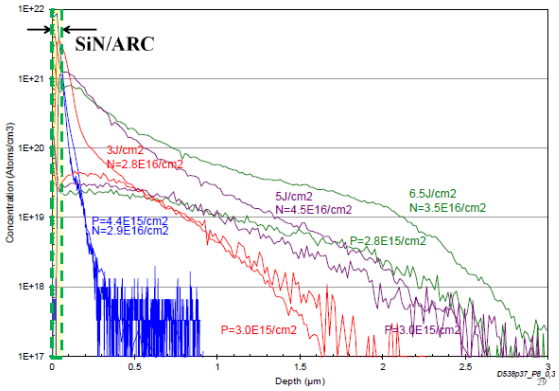

Fig.21: SiN/P-implant N-SIMS areal density analysis.

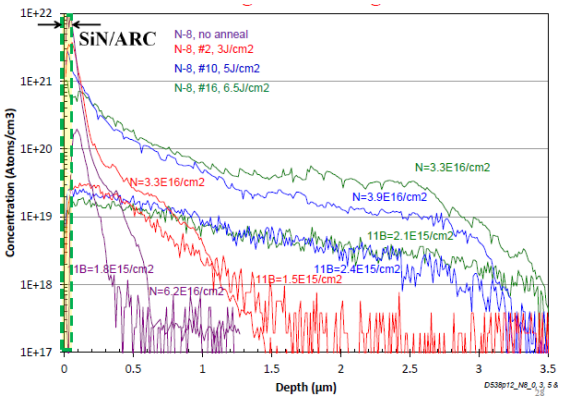

Fig.22: SiN/B-implant N-SIMS areal density analysis.

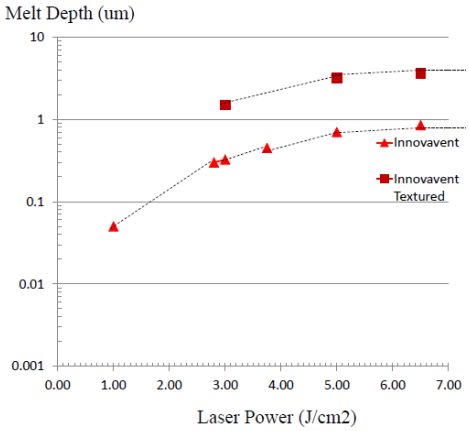

Fig.23: Silicon melt depth versus laser power for polished and textured silicon surfaces.

The SiN/P-implant and SiN/B-implant wafers were RTA annealed for 1 minute by NDL at 650^{o}C, 750^{o}C, 850^{o}C and 950^{o}C to simulate the EF region junction formation. The SiN/P results are shown in Fig.24 while the SiN/B results are shown in Fig.25. The SiN/P Rs values are much higher than P only and microwave annealing had no effect suggesting the SiN/P-implant was not amorphous but rather crystalline so no SPE dopant activation. Rs values for RTA at 650^{o}C, 750^{o}C, 850^{o}C and 950^{o}C were 162Ω/□, 157Ω/□, 122Ω/□ and 86Ω/□ respectively so ideal for EF and a P activated dose of <6E14/cm^2. The SiN/B Rs results on the other hand were similar to the B only case as shown in Fig.25. At 650^{o}C Rs=965Ω/□, at 750^{o}C Rs=390Ω/□, at 850^{o}C Rs=249Ω/□ and at 950^{o}C Rs=91Ω/□.

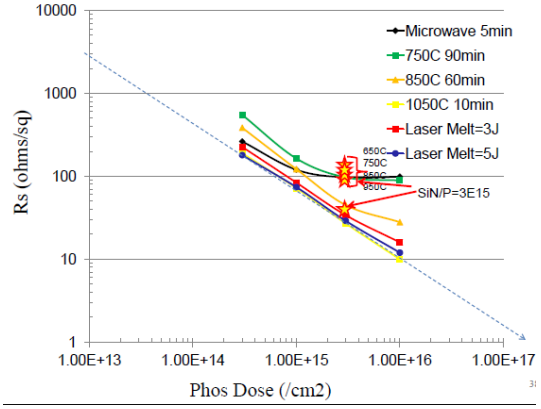

Fig.24: SiN/P-implant Rs versus RTA annealing temperature.

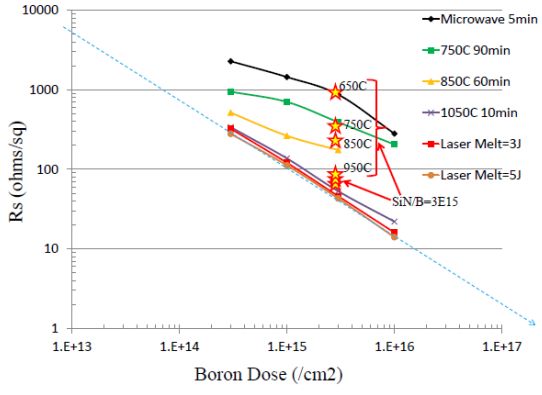

Fig.25: SiN/B-implant Rs versus RTA annealing

temperature.

Fig.26 is a plot of Rs versus annealing temperature condition for P and As dopant in this study while Fig.27 is for B dopant. For $POCl_3$ diffusion doping as shown in Fig.26 the P activated concentration at 850°C is ~2E15/cm^2 and at 1407°C for >3J/cm^2 laser anneal ~5.5E15/cm^2 (also see Fig.7).

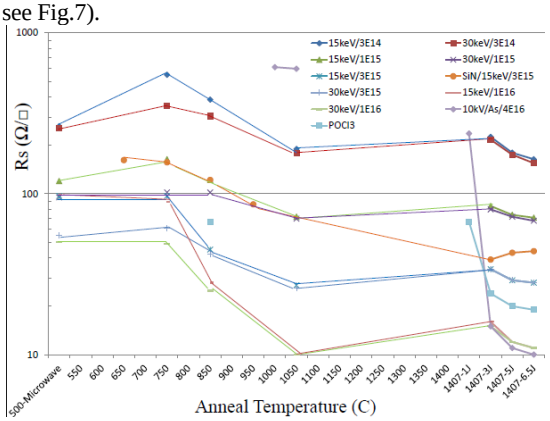

Fig.26: N-type P and As dopant Rs versus annealing temperature condition.

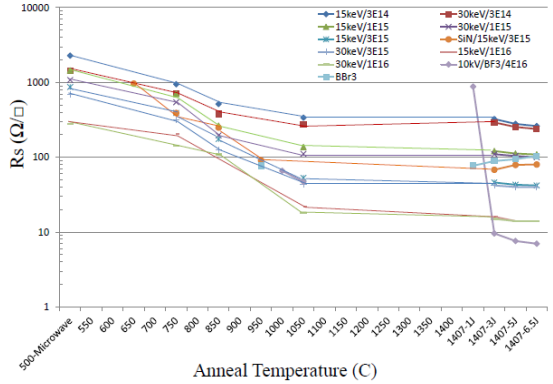

Fig.27: B dopant Rs versus annealing temperature condition.

3.4 Combination of SE laser annealing with either pre-furnace or post-furnace diffusion annealing results.

Fig.28 shows the 3J/cm^2 laser anneal Rs results for 15keV P-implant at 3E15/cm^2 for: 1) laser anneal only, 2) laser anneal with post furnace diffusion anneal and 3) pre-furnace diffusion anneal then laser anneal. Rs for laser only anneal was 35Ω/□ (activated P dose ~3E15/cm^2) and laser + post-furnace anneal Rs was 33Ω/□ (activated P dose ~3E15/cm^2) while pre-furnace + laser anneal Rs was 49Ω/□ (activated P dose ~2E15/cm^2) or ~30% activation degradation. Fig.29 shows the 15keV B-implant results at 1E16/cm^2 dose. Both laser only anneal at 3J/cm^2 and laser + post-furnace anneal Rs=19Ω/□ (B activated dose ~1E16/cm^2) but the pre-furnace + laser Rs=29Ω/□ (B activated dose ~5.5E15/cm^2) or 44% activation degradation. Therefore the best annealing combination is laser anneal first with post-furnace diffusion annealing.

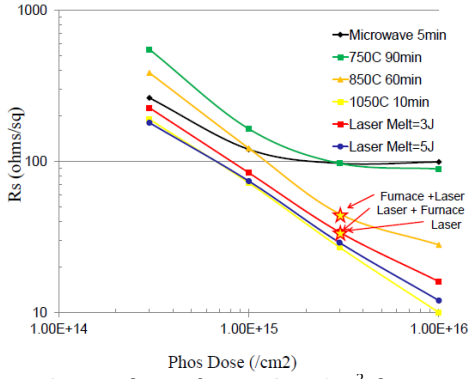

Fig.28: P-implant 15keV at 3E15/cm^2 dose Rs results for laser, laser + post-furnace and pre-furnace + laser annealing sequences.

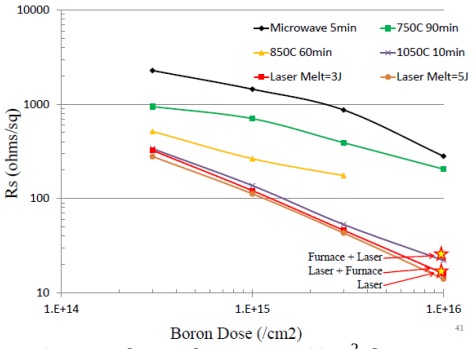

Fig.29: B-implant 15keV at 1E16/cm^2 dose Rs results for laser, laser + furnace and furnace + laser annealing sequences.

4 SUMMARY/CONCLUSION

The P dopant content in $POCl_3$ was ~1.06E16/cm^2 as detected by P-SIMS areal density measurements but only 20% (~2E15/cm^2) was electrically active after the standard 850°C furnace doping process. The 3J/cm^2 laser melt anneal increased the P activated dopant level to 5.5E15/cm^2. However, with P or B implanted dopant, 100% activation was achieved with 3J/cm^2 or higher laser anneals power conditions. With a SiN/ARC surface layer, the SE laser melt annealing step resulted in up to 50% lower dopant activation and we detected high levels of nitrogen incorporation in the melt region between 5E19 to 5E20/cm^3 so further process optimization is required and will be reported in the future. Also, furnace 1st followed by laser anneal resulted in 30-44% lower dopant activation compared to laser 1st then furnace anneal.

5 REFERENCES

[1] J. Borland et al., IEEE-PVSC-2012 paper #626.
[2] M. Nejatiet et al., IEEE-PVSC-2012 paper#882.
[3] M. Burrows et al., IEEE-PVSC-2012 paper#627.
[4] Y. Liu et al., IEEE-PVSC-2012 paper#627.
[5] K. Alberi et al., IEEE-PVSC-2010 paper#334.
[6] H. Antoniadis et al., IEEE-PVSC-2010, paper#276.
[7] U. Jaeger et al., IEEE-PVSC-2010 paper#806.
[8] Z. Shi et al., www.Suntech-power.com web-site Pluto cell white paper.
[9] B. Paviet-Salomon et al., EU-PVSEC-2011, paper 2BV.1.47.
[10] Kennel, IEEE-RTP 2006 conference.
[11] B. Xu et al., IEEE-PVSC-2009, p.517.